

Supporting Information

**Cyclopentadithiophene Organic Core in Small Molecule Organic Solar Cells:
Morphological Control of Carrier Recombination**

Rocío Domínguez,^{a+} Núria F. Montcada,^{b+} Pilar de la Cruz,^a Emilio Palomares^{*b,c} and Fernando Langa^{*a}

^a Institute for Nanoscience, Nanotechnology and Molecular Materials (INAMOL). University of Castilla-la Mancha, Campus de la Fábrica. 45071. Toledo, Spain.

^b Institute of Chemical Research of Catalonia (ICIQ), Avinguda del Països Catalans 16, 43007 Tarragona, Spain. Fax: +34 977 920 823; Tel: +34 977 920 200; E-mail: epalomares@iciq.es

^c Catalan Institution for Research and Advanced Studies (ICREA), Passeig de Lluís Companys 23, 08010 Barcelona, Spain

† These authors contributed equally to this work.

Table of Contents

1.- Experimental conditions.....	S2
2.- ^1H NMR, ^{13}C NMR, IR and MS spectra.....	S3
3.- Thermogravimetric (TGA) and Differential Scanning Calorimetry (DSC) analyses.....	S15
4.- Ciclic Voltammetry (CV) spectra.	S16
6.- Device fabrication and characterization.	S17
7.- Hole only device characterization.	S18

1.- Experimental conditions.

Synthetic procedures were carried out under inert argon atmosphere and in dry solvent unless otherwise noted. All reagents and solvents were reagent grade and were used without further purification. Chromatographic purifications were performed using silica gel 60 SDS (particle size 0.040-0.063 mm). Analytical thin-layer chromatography was performed using Merck TLC silica gel 60 F254. ¹H NMR spectra were obtained on Bruker TopSpin AV-400 (400 MHz) spectrometer. Chemical shifts are reported in parts per million (ppm) relative to the solvent residual peak (CDCl₃, 7.27 ppm). ¹³C NMR chemical shifts are reported relative to the solvent residual peak (CDCl₃, 77.00 ppm). UV-Vis measurements were carried out on a Shimadzu UV 3600 spectrophotometer. For extinction coefficient determination, solutions of different concentration were prepared in CH₂Cl₂, HPLC grade, with absorption between 0.1-1 of absorbance using a 1 cm UV cuvette. Mass spectra (MALDI-TOF) were recorded on a VOYAGER DETTM STR mass spectrometer using dithranol as matrix. Melting points are uncorrected. Cyclic voltammetry was performed in o-dichlorobenzene/acetonitrile 4:1 solutions. Tetrabutylammonium perchlorate (0.1 M as supporting electrolyte) was purchased from Acros and used without purification. Solutions were deoxygenated by argon bubbling prior to each experiment which was run under argon atmosphere. Experiments were done in a one-compartment cell equipped with a glassy carbon working electrode ($\varnothing = 2$ mm) and a platinum wire counter electrode. An Ag/AgNO₃ (0.01 M in the supporting electrolyte) electrode was used as reference and checked against the ferrocene/ferrocenium couple (Fc/Fc⁺) before and after each experiment.

Thermogravimetric analyses were performed using a TGA/DSC Linea Excellent instrument by Mettler-Toledo and collected under inert atmosphere of nitrogen with a scan rate of 10°C min⁻¹. The weight changes were recorded as a function of temperature. Differential scanning calorimetry analyses were performed by a DSC Linea Excellent instrument by Mettler-Toledo, and collected under inert atmosphere of nitrogen at a heating rate of 20 K/min and a cooling rate of 10 K/min.

The molecular geometries and frontier molecular orbitals of these new molecules have been optimized by density functional theory (DFT) calculations at the B3LYP/6-31G* level.¹

¹ Gaussian 09, Frisch, M. J.; Trucks, G. W.; Schlegel, H. B.; Scuseria, G. E.; Robb, M. A.; Cheeseman, J. R.; Montgomery Jr., J. A.; Vreven, T.; Kudin, K. N.; Burant, J. C.; Millam, J. M.; Iyengar, S. S.; Tomasi, J.; Barone, V.; Mennucci, B.; Cossi, M.; Scalmani, G.; Rega, N.; Petersson, G. A.; Nakatsuji, H.; Hada, M.; Ehara, M.; Toyota, K.; Fukuda, R.; Hasegawa, J.; Ishida, M.; Nakajima, T.; Honda, Y.; Kitao, O.; Nakai, H.; Klene, M.; Li, X.; Knox, J. E.; Hratchian, H. P.; Cross, J. B.; Bakken, V.; Adamo, C.; Jaramillo, J.; Gomperts, R.; Stratmann, R. E.; Yazyev, O.; Austin, A. J.; Cammi, R.; Pomelli, C.; Ochterski, J. W.; Ayala, P. Y.; Morokuma, K.; Voth, G. A.; Salvador, P.; Dannenberg, J. J.; Zakrzewski, V. G.; Dapprich, S.; Daniels, A. D.; Strain, M. C.; Farkas, O.; Malick, D. K.; Rabuck, A. D.; Raghavachari, K.; Foresman, J. B.; Ortiz, J. V.; Cui, Q.; Baboul, A. G.; Clifford, S.; Cioslowski, J.; Stefanov, B. B.; Liu, G.; Liashenko, A.; Piskorz, P.; Komaromi, I.; Martin, R. L.; Fox, D. J.; Keith, T.; Al-Laham, M. A.; Peng, C. Y.; Nanayakkara, A.; Challacombe, M.; Gill, P. M. W.; Johnson, B.; Chen, W.; Wong, M. W.; Gonzalez, C.; Pople, J. A. Gaussian, Inc., Wallingford CT, 2004.

2.- ^1H NMR, ^{13}C NMR, IR and MS spectra.

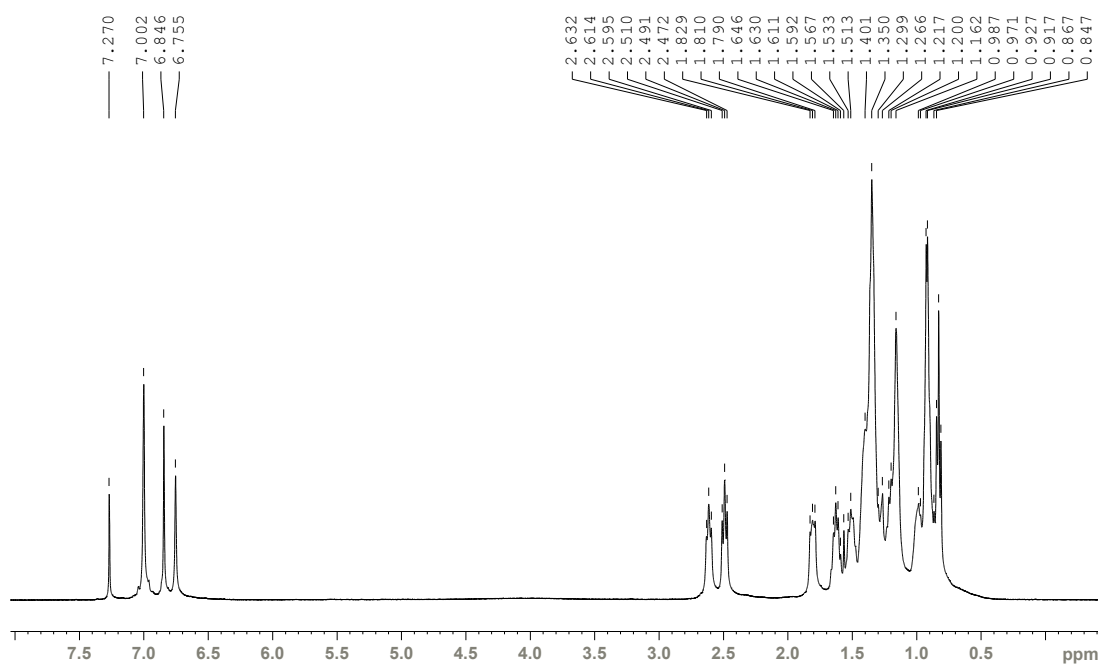


Figure S1. ^1H NMR spectrum (400 MHz, CDCl_3) of **4**.

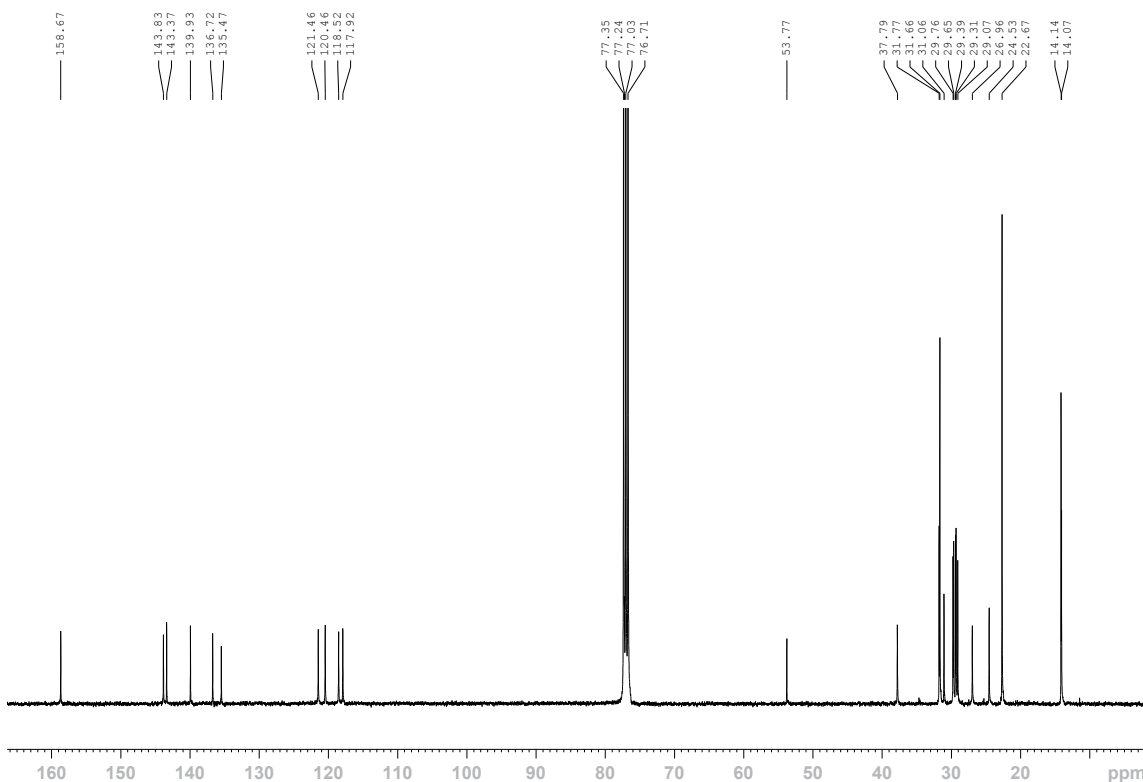


Figure S2. ^{13}C NMR spectrum (100 MHz, CDCl_3) of **4**.

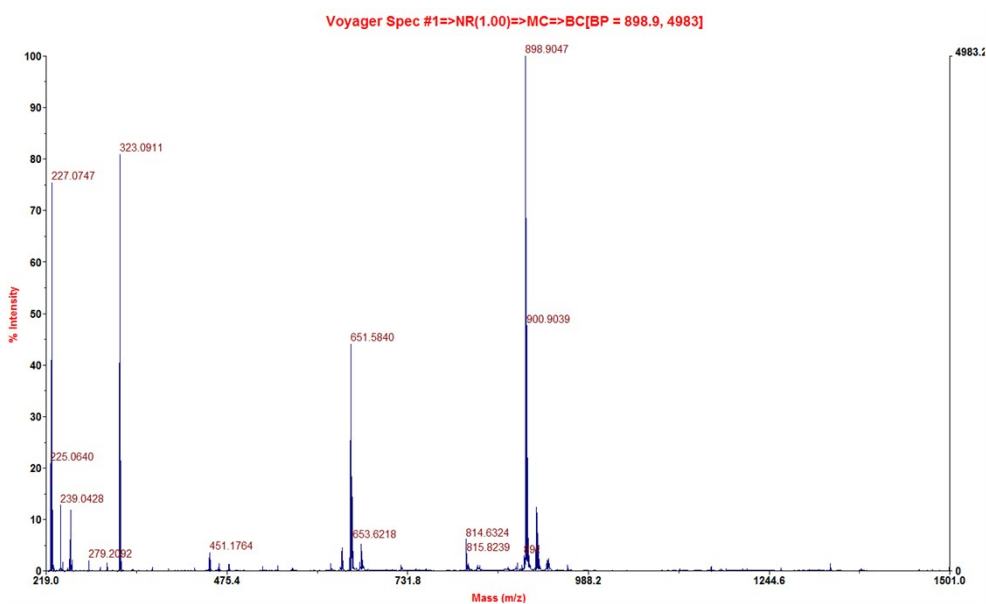


Figure S3. MALDI-MS spectrum of **4** (Matrix: Dithranol).

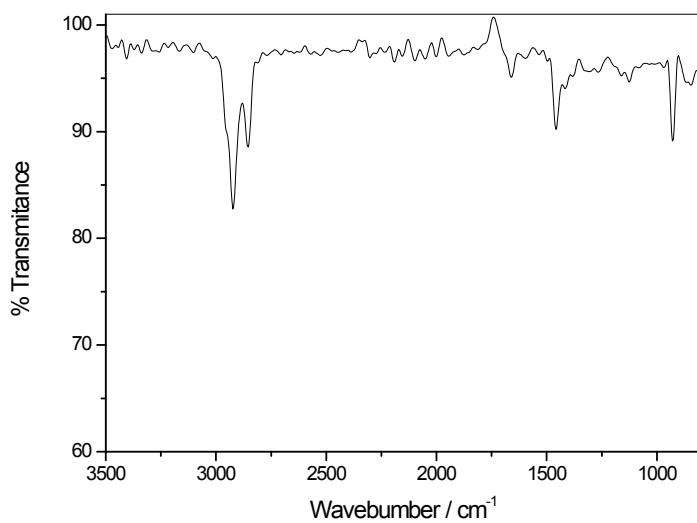


Figure S4. FT-IR spectrum of **4**.

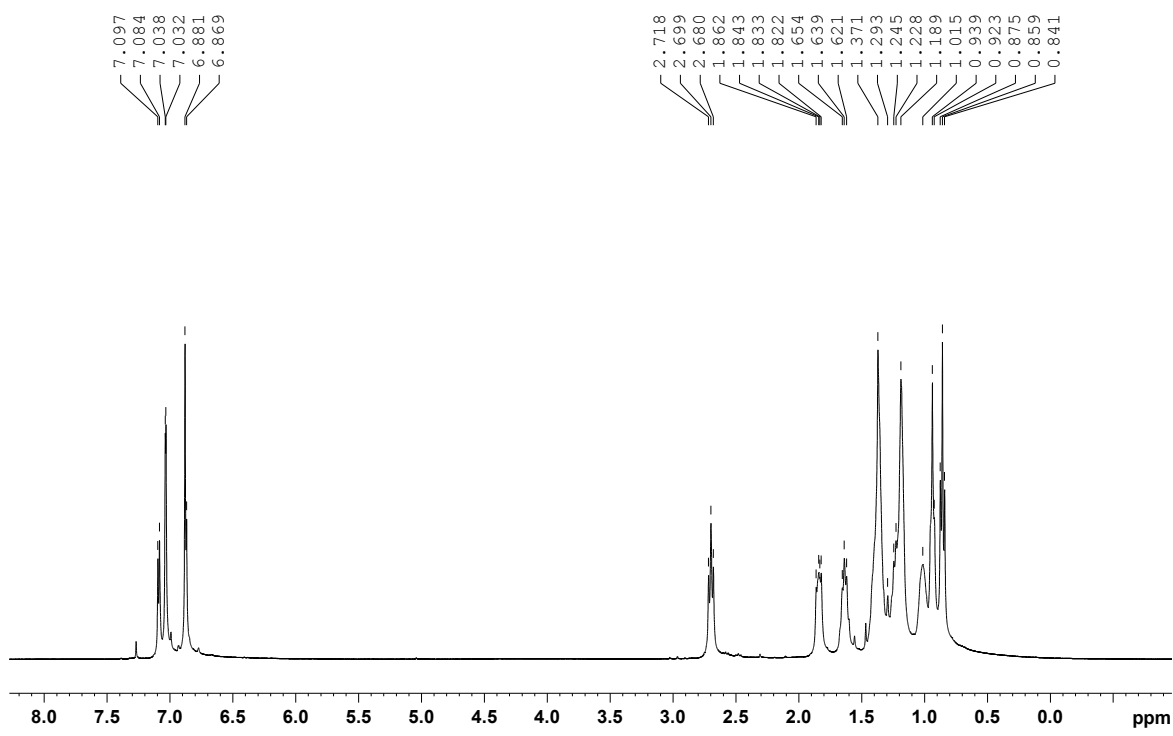


Figure S5. ^1H NMR spectrum (400 MHz, CDCl_3) of **5**.

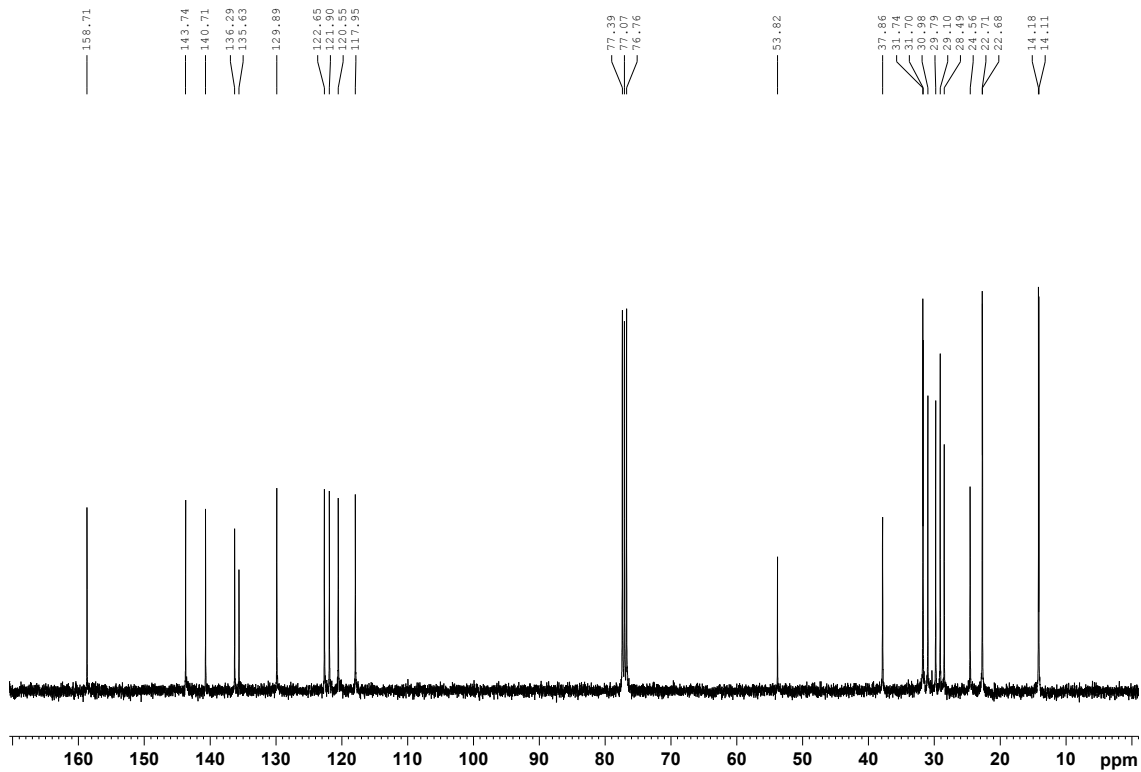


Figure S6. ^{13}C NMR spectrum (100 MHz, CDCl_3) of **5**.

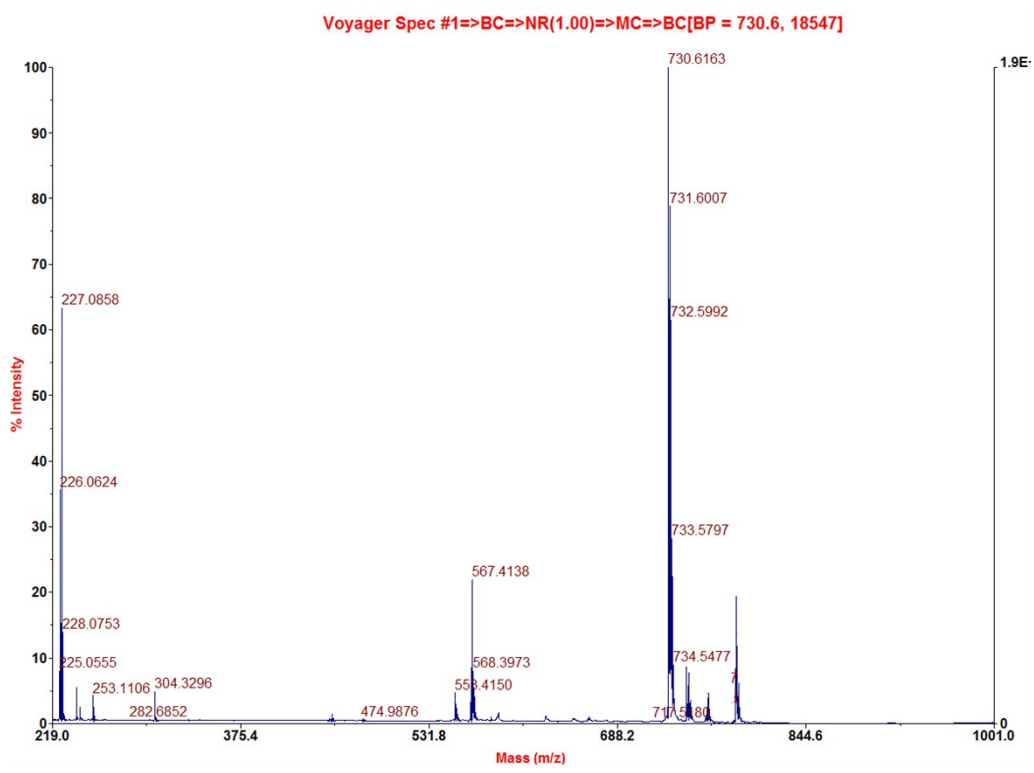


Figure S7. MALDI-MS spectrum of **5** (Matrix: Dithranol).

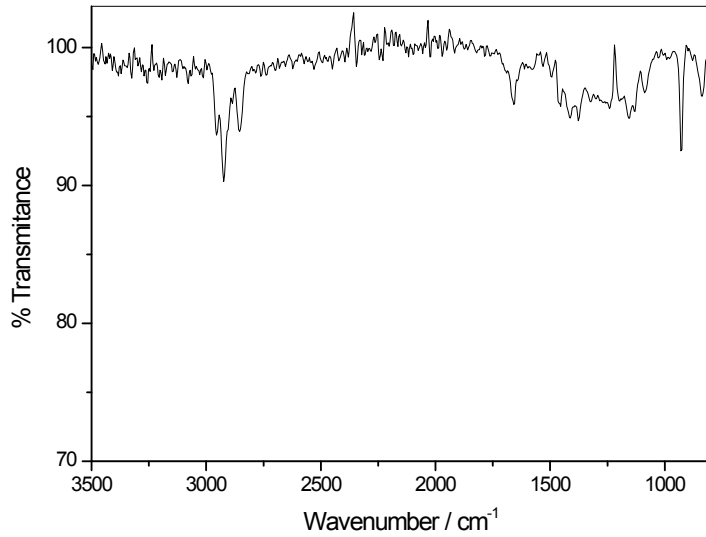


Figure S8. FT-IR spectrum of **5**.

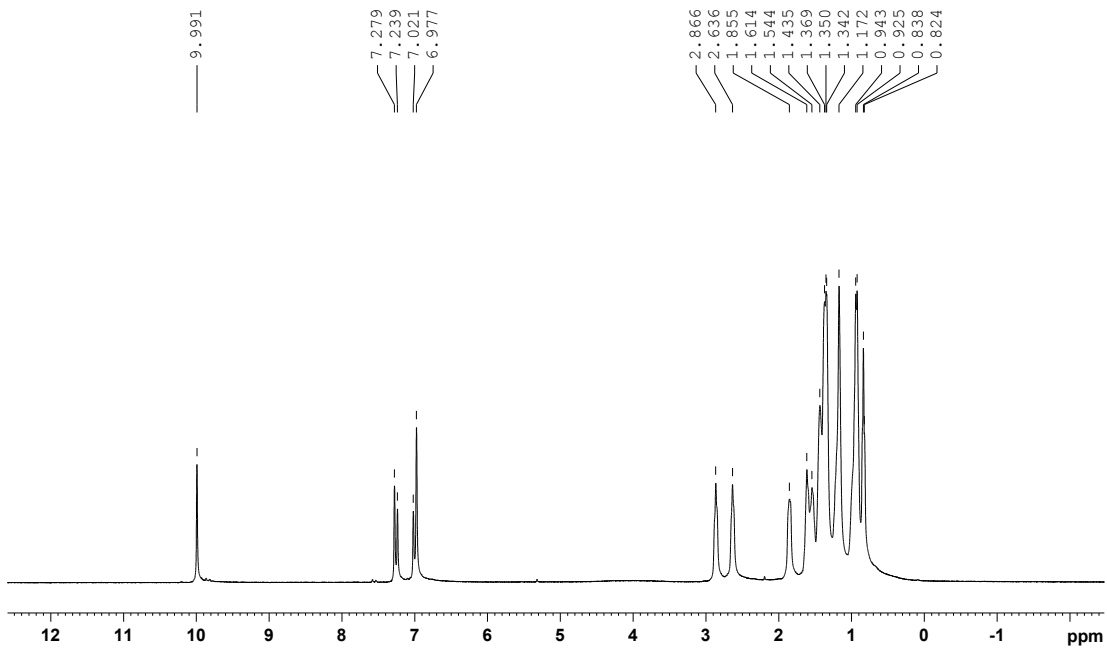


Figure S9. ^1H NMR spectrum (400 MHz, CDCl_3) of **6**.

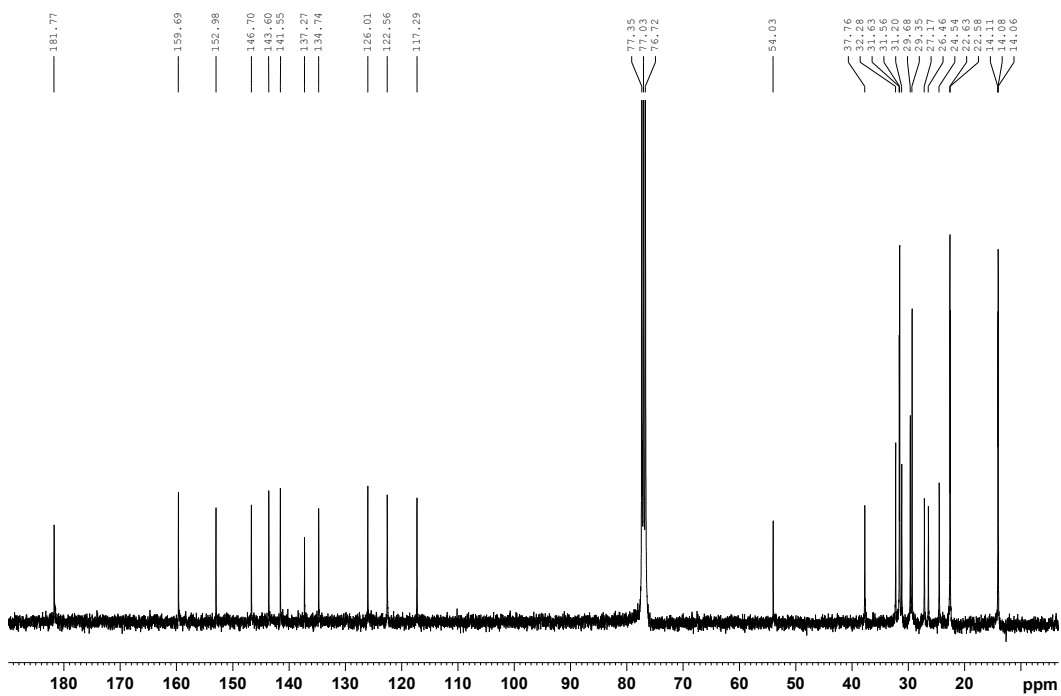


Figure S10. ^{13}C NMR spectrum (100 MHz, CDCl_3) of **6**.

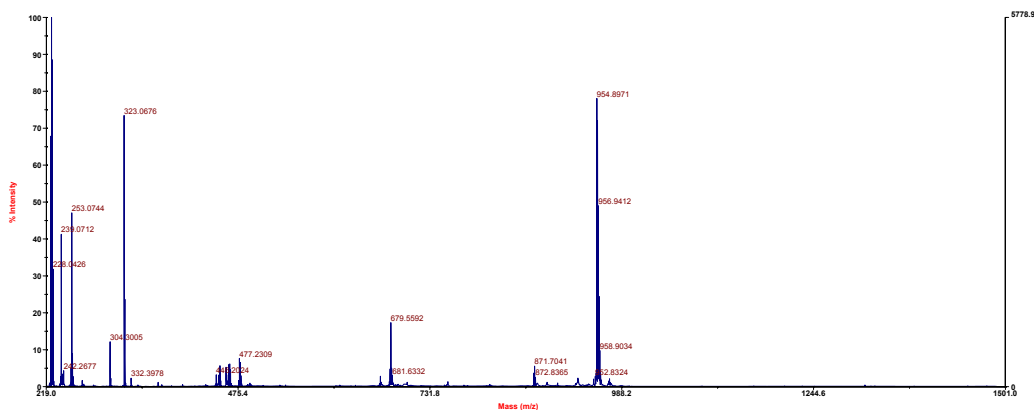


Figure S11. MALDI-MS spectrum of **6** (Matrix: Dithranol).

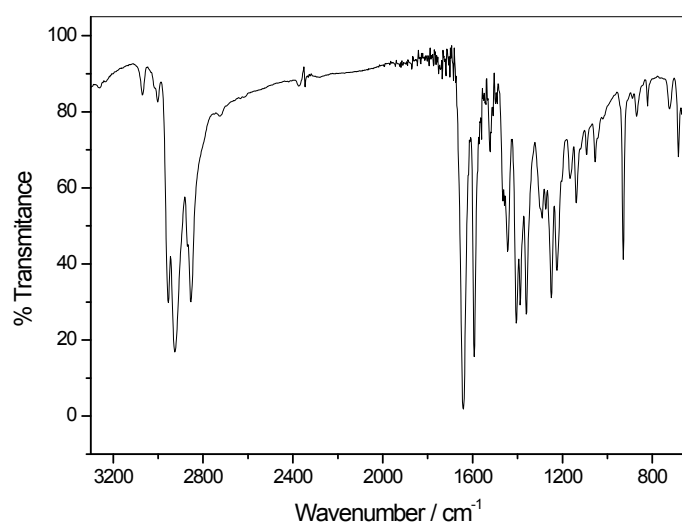


Figure S12. FT-IR spectrum of **6**.

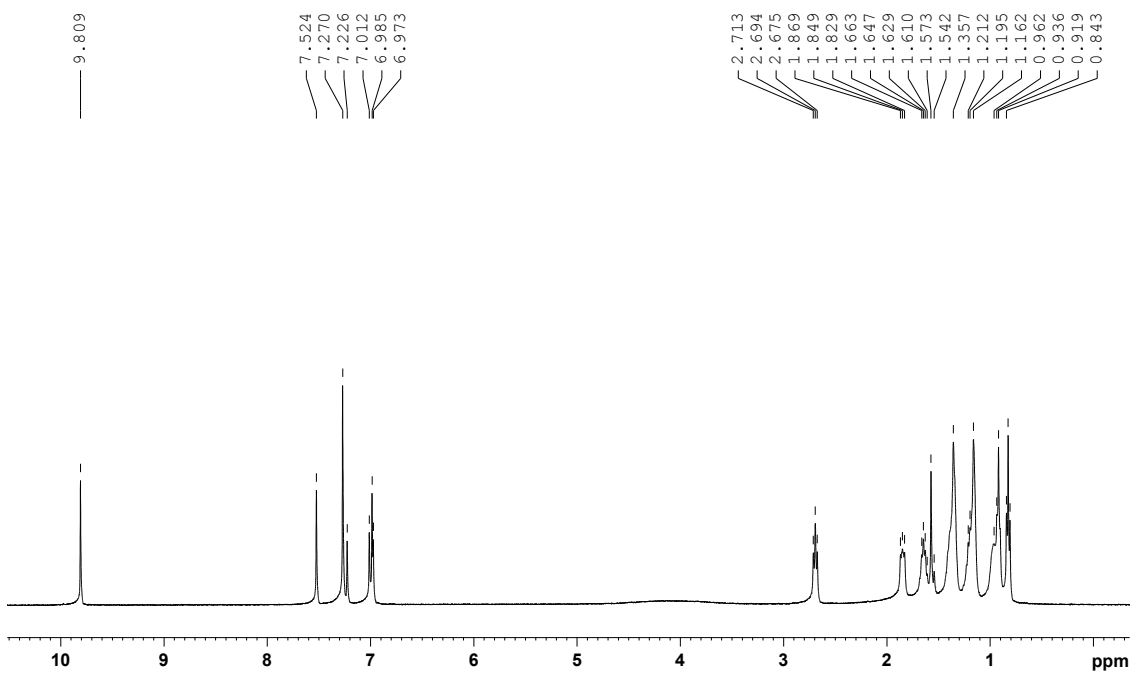


Figure S13. ^1H NMR spectrum (400 MHz, CDCl_3) of **7**.

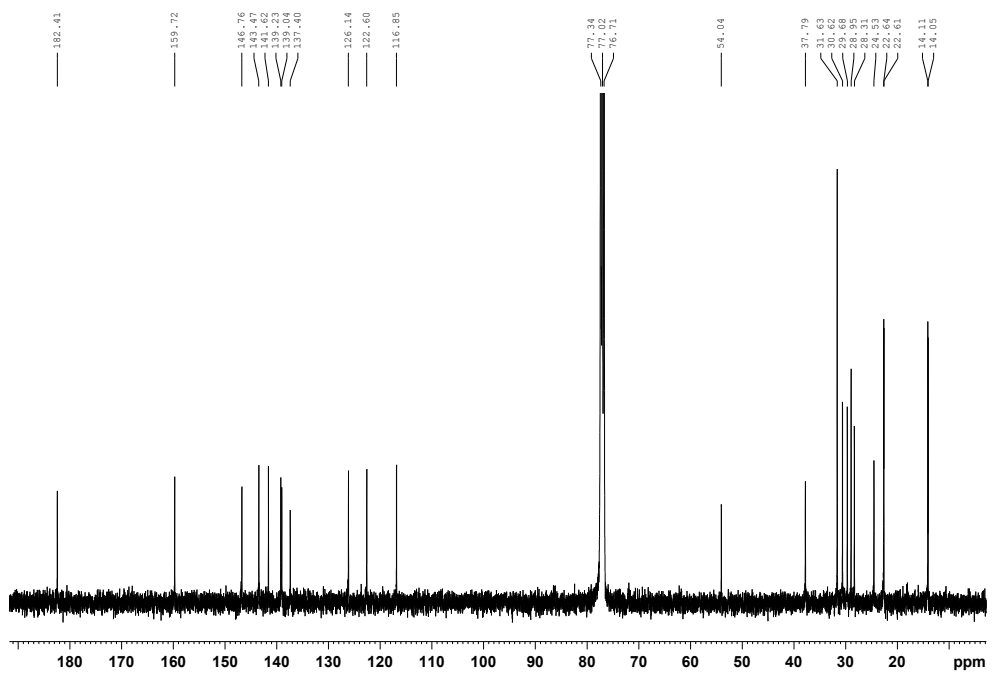


Figure S14. ^{13}C NMR spectrum (100 MHz, CDCl_3) of **7**.

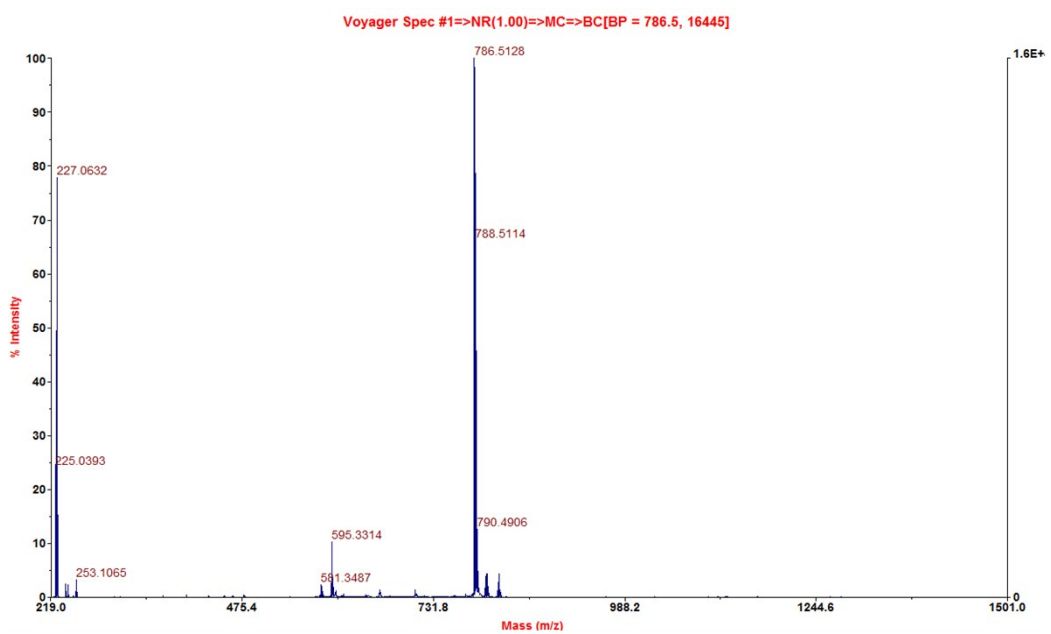


Figure S15. MALDI-MS spectrum of **7** (Matrix: Dithranol).

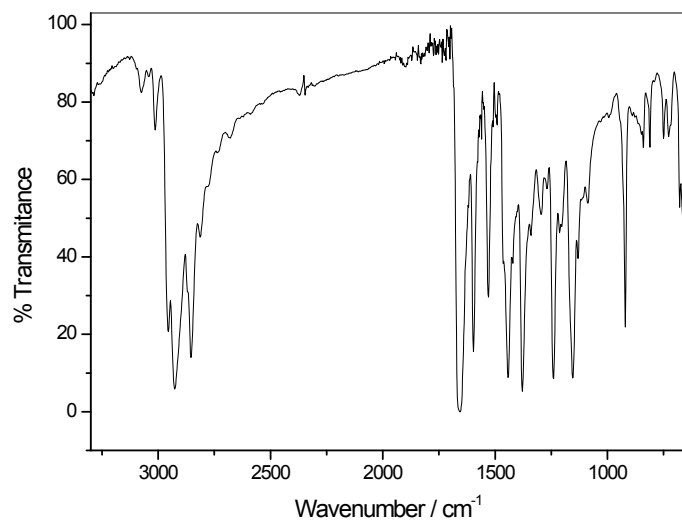


Figure S16. FT-IR spectrum of **7**.

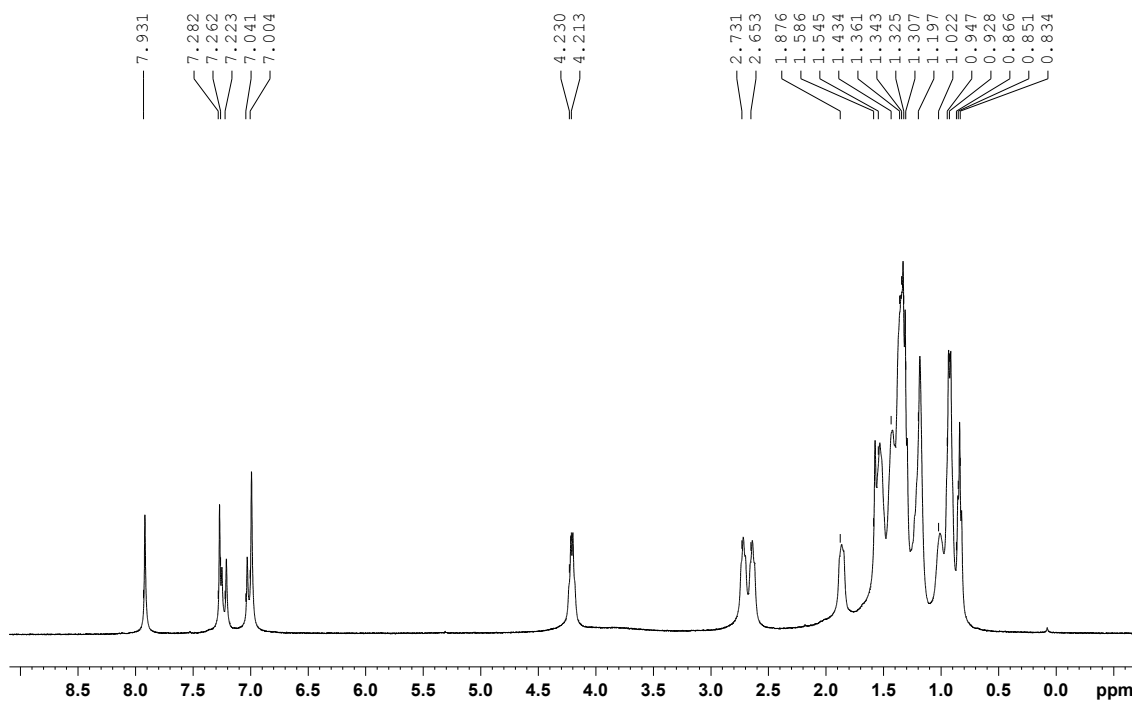


Figure S17. ¹H NMR spectrum (400 MHz, CDCl₃) of RD5.

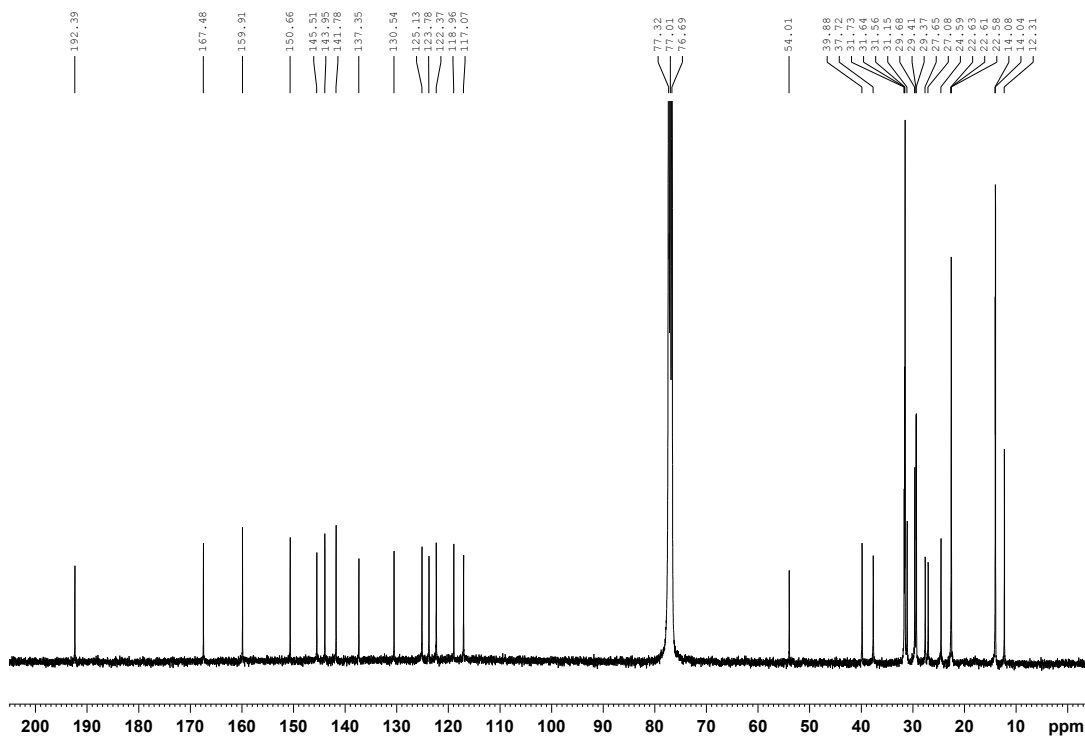


Figure S18. ¹³C NMR spectrum (100 MHz, CDCl₃) of RD5.

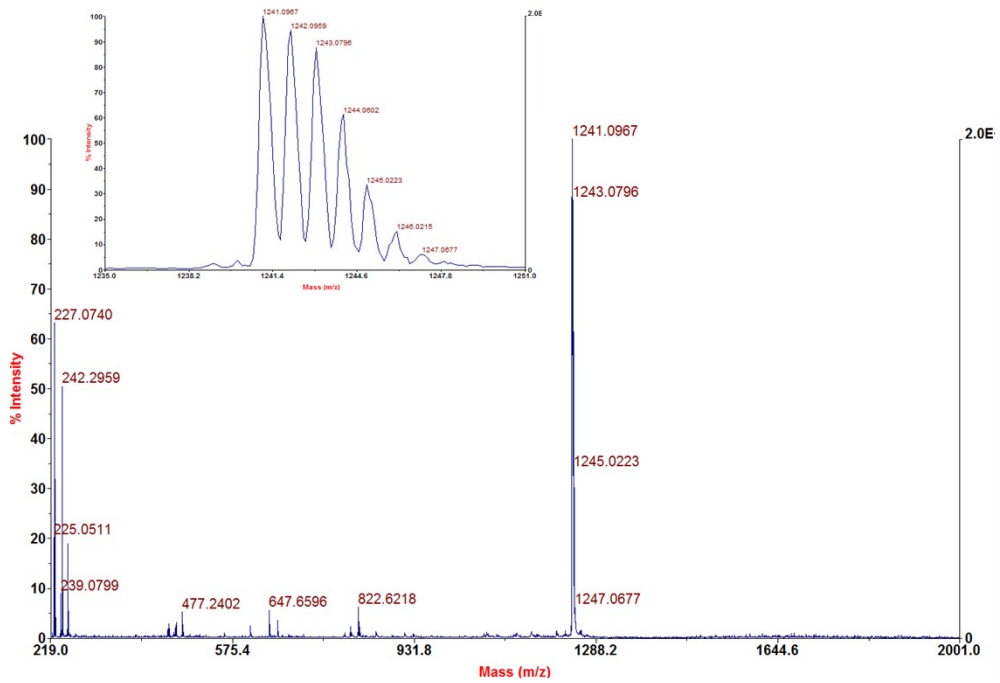


Figure S19. MALDI-MS spectrum of RD5 (Matrix: Dithranol).

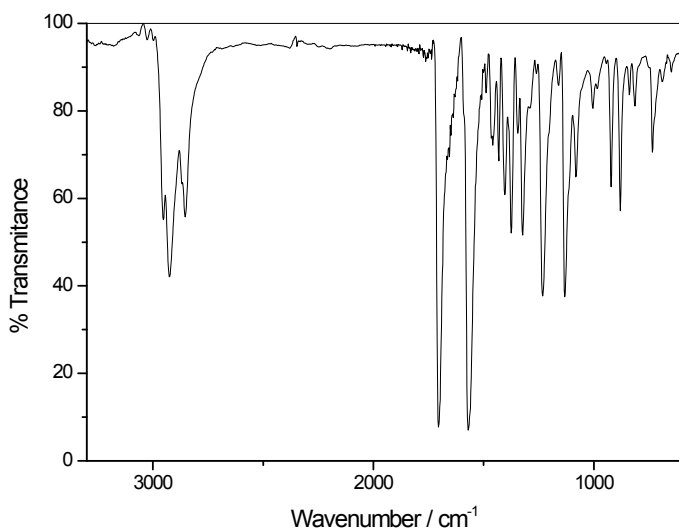


Figure S20. FT-IR spectrum of RD5.

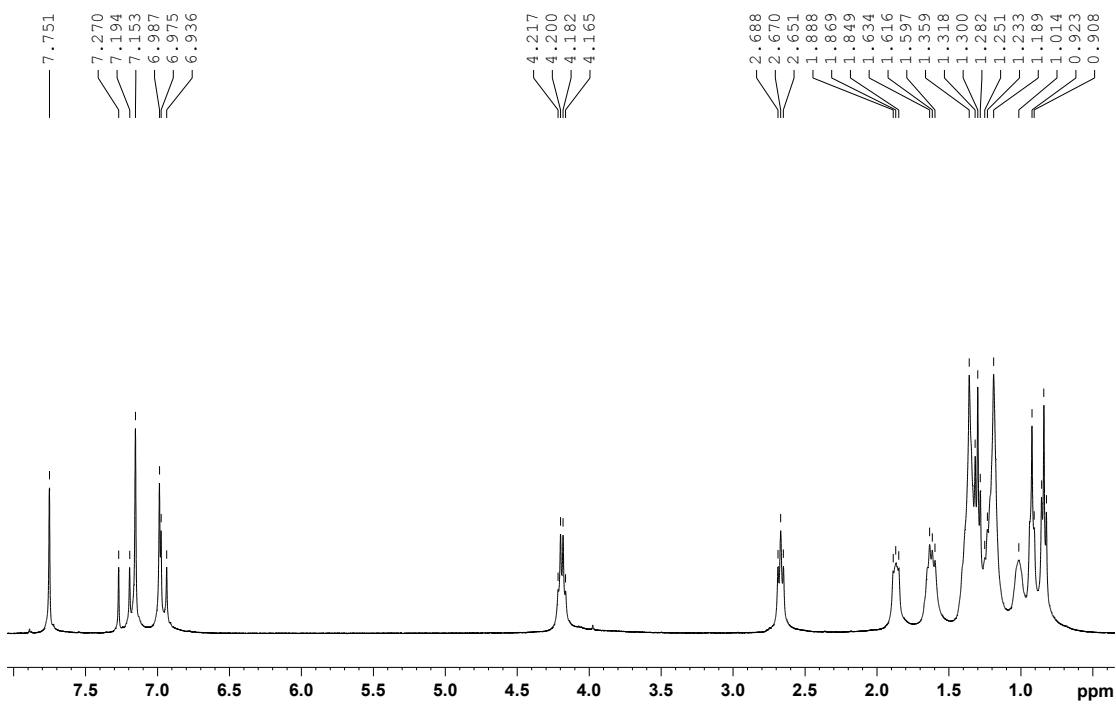


Figure S21. ¹H NMR spectrum (400 MHz, CDCl₃) of RD6.

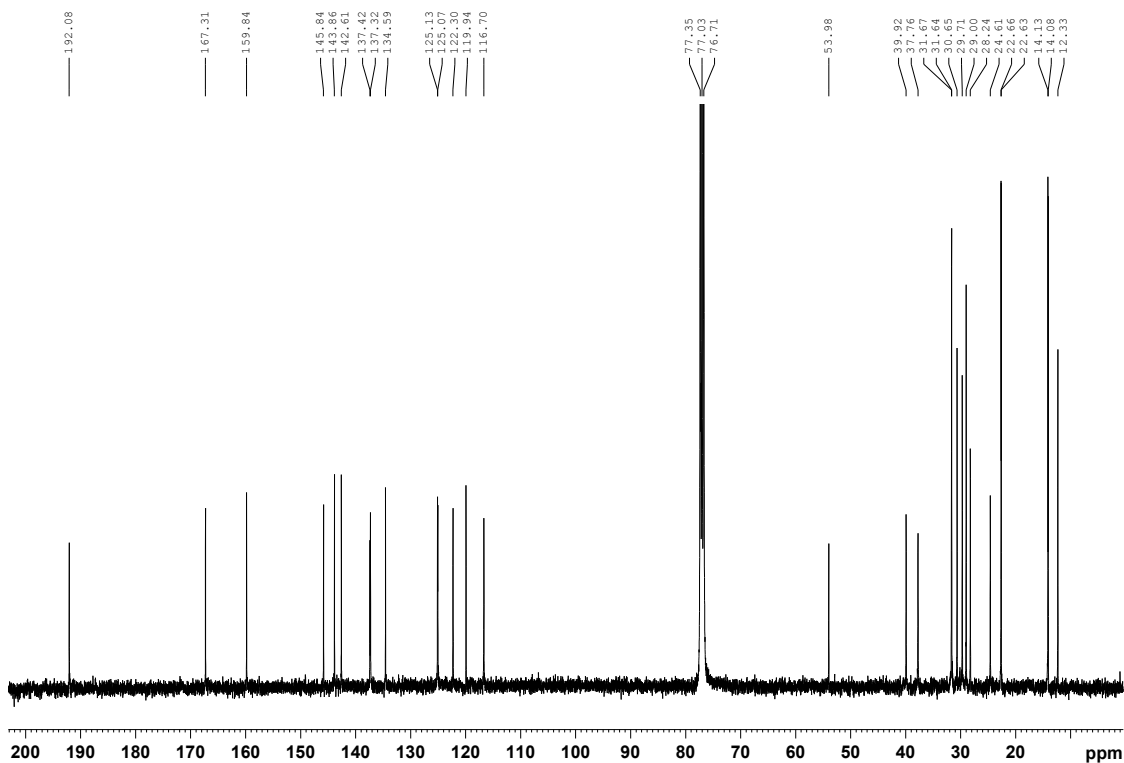


Figure S22. ¹³C NMR spectrum (100 MHz, CDCl₃) of RD6.

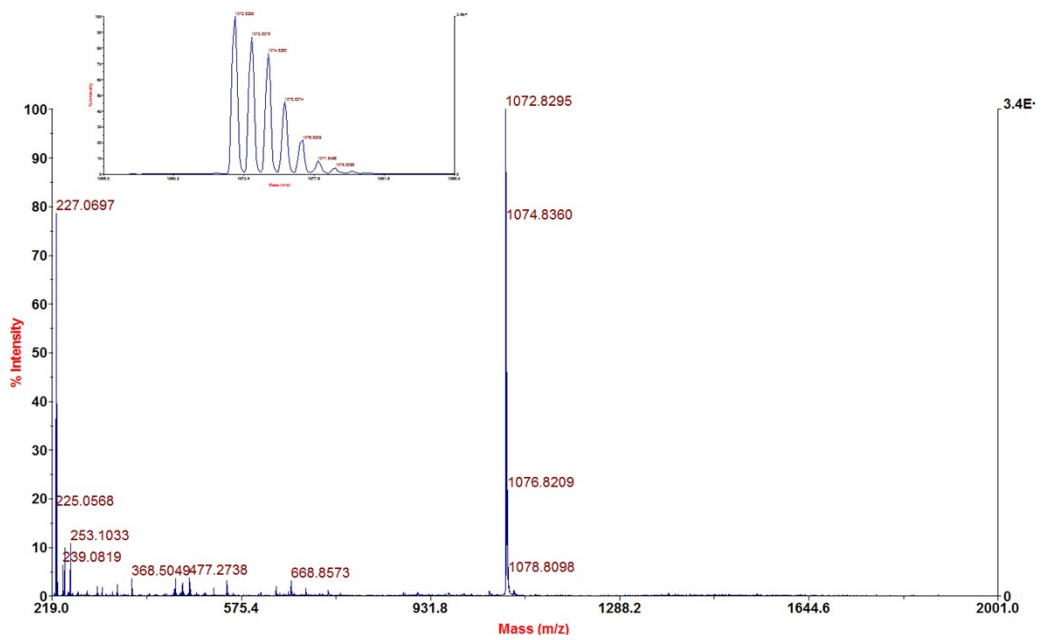


Figure S23. MALDI-MS spectrum of **RD6** (Matrix: Dithranol).

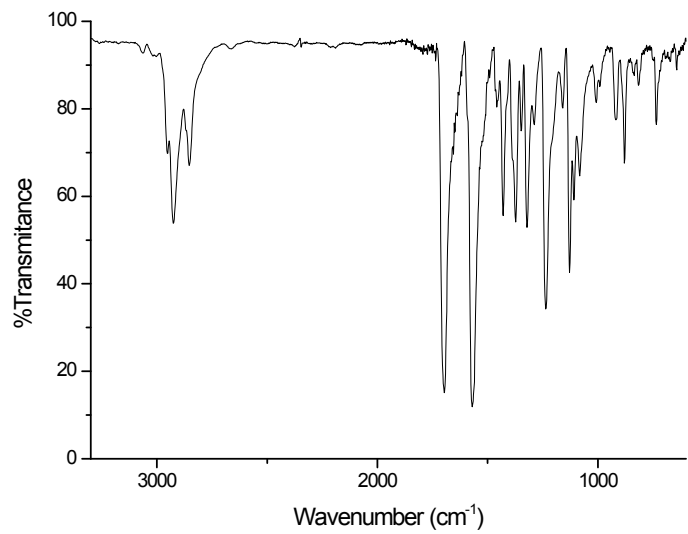


Figure S24. FT-IR spectrum of **RD6**.

3.- Thermogravimetric (TGA) and Differential Scanning Calorimetry (DSC) analyses.

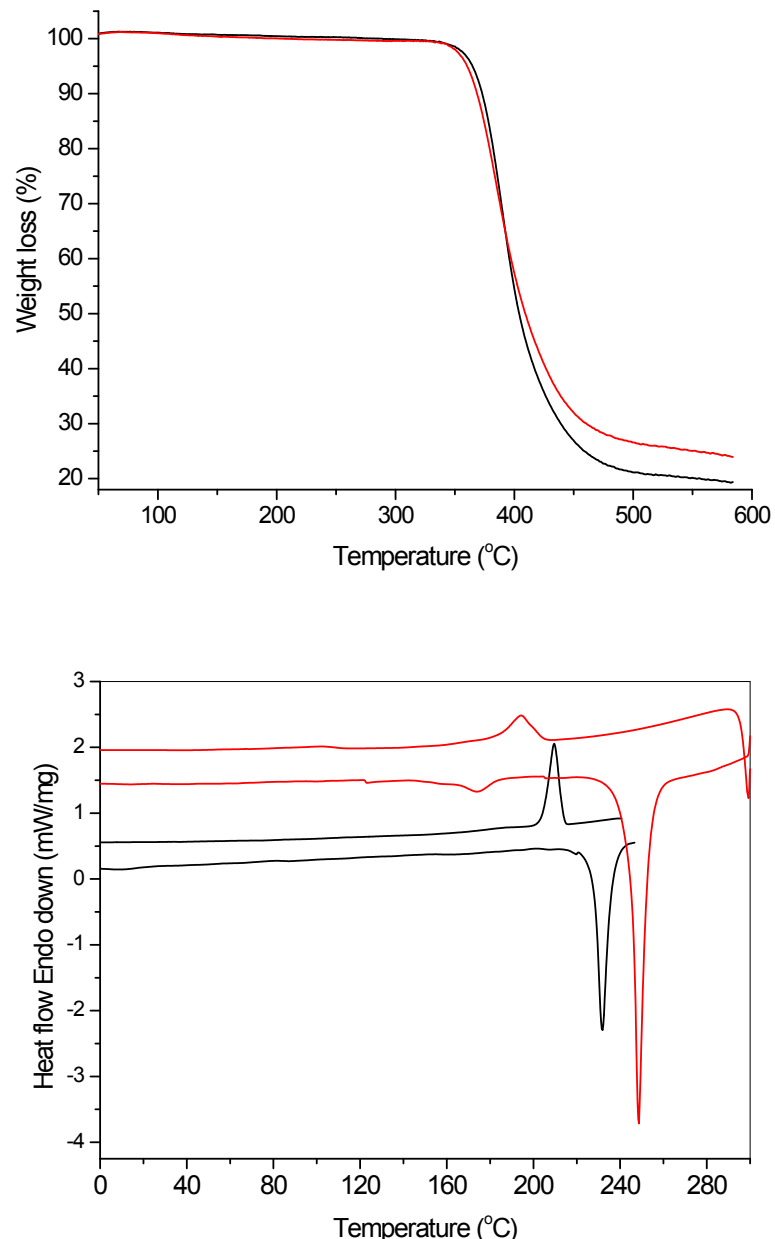


Figure S25. (up) TGA and (down) DSC curves of **RD5** (black line) and **RD6** (red line) at scan rate of $10^{\circ}\text{C min}^{-1}$.

4.- Ciclic Voltammetry (CV) spectra.

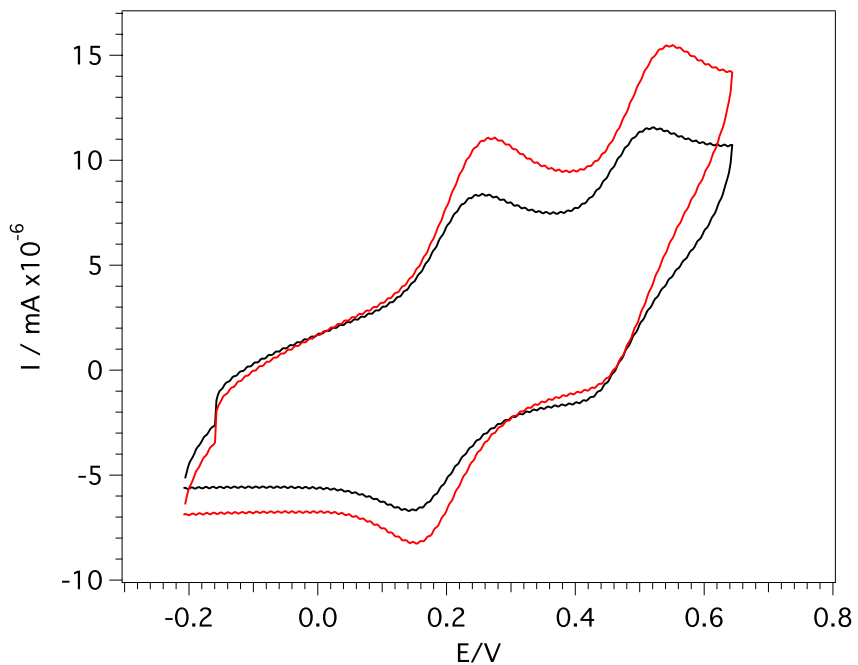


Figure S26. Cyclic voltammograms of **RD5** (black line) and **RD6** (red line) (referred to Fc/Fc⁺).

5.- Theoretical Calculations

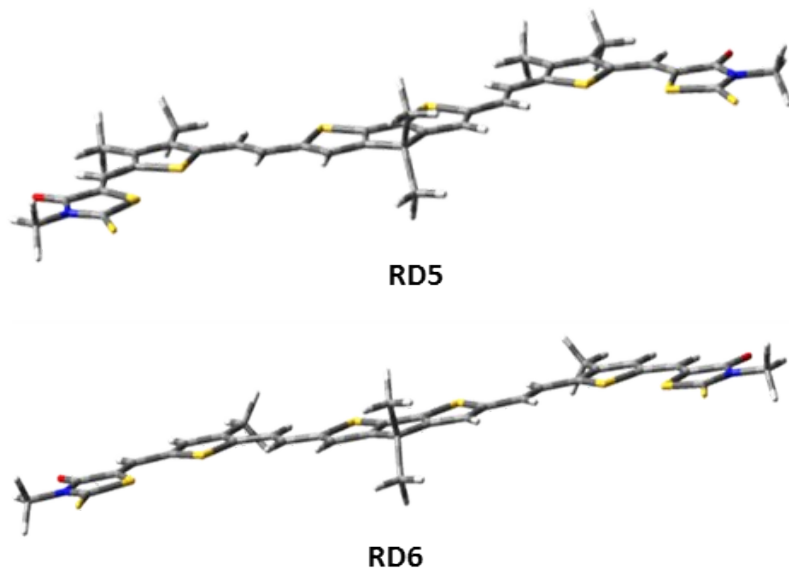


Figure S27. Optimized ground-state geometries of oligomers **RD5** and **RD6**.

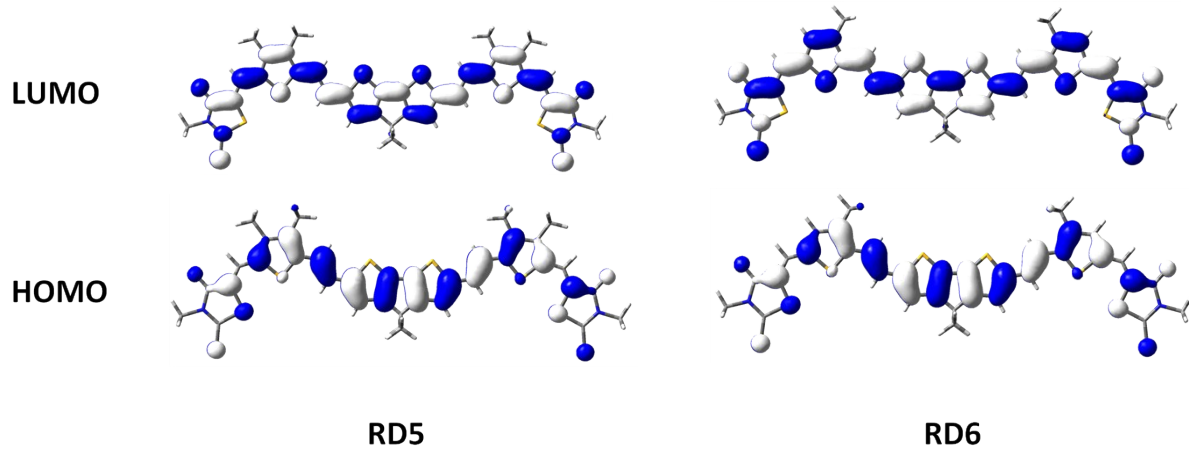


Figure S28. Electronic distribution of the HOMO and LUMO energy levels in **RD5** and **RD6**.

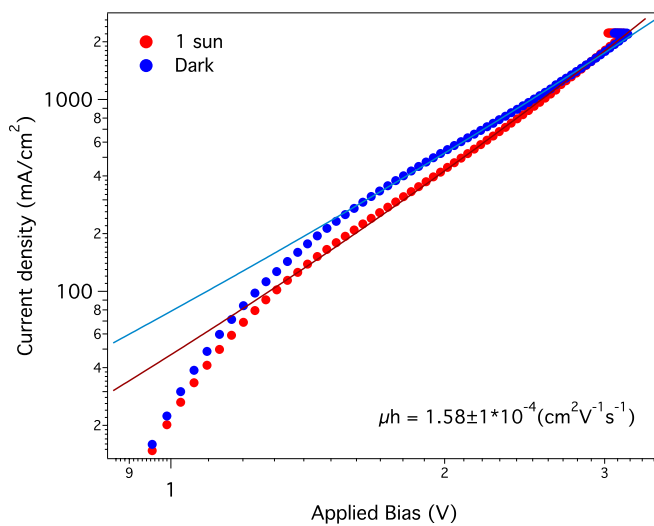
6.- Device fabrication and characterization.

All devices used in this study were fabricated using ITO coated glass substrates ($5 \Omega/\text{cm}^2$) were ultrasonically cleaned consecutively in acetone and two times in isopropyl alcohol, and dried under a nitrogen flow. Substrates were treated in a UV-ozone cleaner for 30 min in ambient atmosphere. An aqueous solution of Poly(3,4-ethylenedioxythiophene):poly(styrenesulfonate) (PEDOT:PSS, from HC StarckBaytron P.) was spin-coated over the ITO substrates to obtain a film of about 25 nm (30s at 4500 rpm in a first step and 30s at 3500 rpm in the second step). The PEDOT/PSS film was dried at 120°C for 15 minutes under inert conditions. A 20 mg/mL (total concentration) solution of RD5 and RD6 was prepared in chloroform with a ratio 1:2 (optimized conditions) with PC₇₁BM and spin-coated over the PEDOT:PSS layer at 8000 rpm obtaining a 100 nm active layer. The solvent annealing was carried out immediately after the active layer deposition, this treatment was performed by exposing the films to a saturated vapor atmosphere of dichloromethane (10 mL) in a controlled volume closed vessel (100 mL) for different periods of time, being 5 and 4 minutes for **RD5** and **RD6**, respectively, the optimized annealing time. Finally, 80 nm Al electrode was thermally evaporated on the active layer in an ultra-high vacuum chamber ($1 \times 10^{-6} \text{ mbar}$), a shadow mask was also used in this step in order to obtain devices with an area of 9 mm^2 . For hole only devices the fabrication were performed following same procedure as described before but using ITO/PEDOT:PSS/donor:PC71BM/Au (150 nm) architecture.

For device characterization, the UV-Vis absorption spectra of films were measured using a Shimadzu UV-1700 spectrophotometer. The J-V characteristics of the devices were measured using a Sun 2000 Solar Simulator (150 W, ABET Technologies) at 100 mW cm⁻² calibrated silicon photodiode (NREL). The appropriate filters were utilized to faithfully simulate the AM 1.5G spectrum. The applied potential and cell current were measured with a Keithley 2400 digital source meter. The current to voltage (J-V curve) was plotted automatically with a home-built Labview© software. The thickness of the films was measured with a stylus profilometer Ambios Tech. XP-1.

7.- Hole only device characterization.

a)



b)

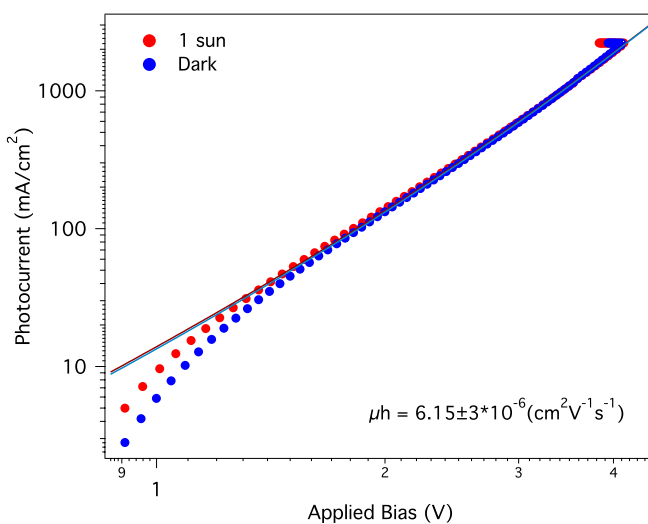


Figure S29. 6 J-V curves for the hole only device of RD5 (a) and RD6 (b) at 1 sun (red) and dark (blue); the solid lines represent the fitting to Mott-Gurney equation.